

HIGH-RESOLUTION PYROMETERS FOR THERMOPHYSICAL SCIENTIFIC EXPERIMENTS

V. N. Senchenko¹, V. S. Dozhikov¹, and D. I. Kapustin¹

¹Associated Institute for High Temperatures of the Russian Academy of Sciences,
Pyrolab Ltd., Moscow, Russia

¹Correspondence should be addressed V. N. Senchenko.

E-mail: pyrolab@ihed.ras.ru

ABSTRACT.

An accurate temperature measurement is of a great importance in most modern researches on thermophysical properties of materials. Two high-resolution automatic pyrometers for real-time monitoring of surface temperature during single-crystal growth from a melt are described. The developed pyrometers measure temperature in a wide dynamic temperature range from 600 to 1500 °C at a typical resolution of 20 mK, and a response time up to 5 ms. The main details of the pyrometers' design, calibration and performance are presented.

KEY WORDS: high-resolution pyrometer, bicolour pyrometer, line scanning pyrometer, single-crystal growth, supercooling.

1. INTRODUCTION

In many cases, contact with a sample is either not possible or not desirable, because it may significantly change sample temperature. Therefore, a precision technique for non-contact temperature measurements is required [1, 2]. Real-time monitoring of surface supercooling temperature in thermophysical experiments during semi-transparent single-crystal growth from a melt involves significant difficulties. These difficulties are caused by the following process parameters: duration of such experiments (more than several hours); small change in the temperature (0.1 – 3.0 °C); wide temperature range (600-1500 °C); small size of a measurement zone (0.5-1.0 mm). Two different high-resolution automatic optical pyrometers have been designed to overcome this problem.

A wide group of dielectric single crystals such as $\text{Bi}_4\text{Ge}_3\text{O}_{12}$, $\text{Bi}_4\text{Si}_3\text{O}_{12}$, $\text{Bi}_4\text{Ge}_3\text{O}_{12}$, $\text{Bi}_{12}\text{GeO}_{20}$, and $\text{Bi}_{12}\text{SiO}_{20}$ grow from the melt by the faceted growth mechanism. Therefore, it is very important to understand how the nature of this mechanism influences the quality of dielectric single crystals. Data on the dependence of the facet supercooling value ΔT upon the growth rate V , the impurity quality and its composition, and the crystallographic direction are required to determine fundamentals of the interface kinetics. The supercooling measurement is based on determination of the thermal radiation intensity of the interface by a high-resolution optical pyrometer viewed through the growing crystal under conditions of an axial heat flux close to the melt-crystal interface (AHP growth method) [3]. The method is based on the peculiar optical properties of the melt and crystal. The absorptivity of the single crystal, k_c , at the melting point in the spectral range 0.5 to 4.0 μm is 0.03 cm^{-1} , and the absorptivity of the melt, k_m , is higher than 200 cm^{-1} . Therefore, one can consider the crystal to be transparent and the melt to be opaque in the spectral range 0.5 to 4.0 μm . In accordance with the method, ΔT is found from the equation: $\Delta T = T_b^m - T_b^v$, where T_b^m is the brightness temperature measured in the absence of growth and corresponded to the melting point, T_b^v is the brightness temperature at the growth rate V corresponded to the temperature of the supercooled interface.

Because the difference between temperature values of the supercooling melt-crystal boundary at various growth rates is small, special high-resolution pyrometers were developed for this experiment.

2. PYROMETER FOR MEASUREMENT OF TEMPERATURE DISTRIBUTION.

The specialized line scanning pyrometer (LSP-I) for measurement of the distribution of “effective” brightness temperature along the melt-crystal interface was developed and manufactured. This pyrometer has high temperature resolution of (10-50) mK, which is sufficient to measure small supercooling. Due to high resolution the pyrometer can determine the difference of interface supercooling at variations of the growth rate and some other parameters. The pyrometer measures brightness temperature at twenty points across melt-crystal interface. Temperature resolution depends on measuring temperature, typical value is 20 mK. The brightness temperature measured in narrow bandwidth at the wavelength - $\lambda_p = 0.827 \mu\text{m}$, which can be changed in the range 0.6–1.1

μm by replacing the filter. The main characteristics of the pyrometer are presented in table 1.

The build-in microcontroller is used for control of pyrometer electronic and for data communication between personal computer and pyrometer via standard RS232 serial interface. The internal data acquisition system of pyrometer one can by programming for temperature monitoring in rates of 0.1-30 measurements per seconds. Special software package was designed for Personal Computer under Windows 2000/XP and allow through program menu choose instrument measurement mode, store data on hard disk and calibrate the pyrometer.

To provide simultaneous temperature measurements of all 20 channels, the internal data acquisition system were used separate analog-to-digital converters (ADC) for each channel. The brightness temperature measured in narrow bandwidth 26 nm at the wavelength - $\lambda_p = 0.827 \mu\text{m}$ that ensured small errors due to changing of “effective” wavelength in whole temperature range. High signal to noise ratio and long term stability in electronic and optic allow reach resolution of (10-50) mK in temperature measurements. Therefore matching in temperature measurements between channels are defined by blackbody quality that used for the pyrometer calibration, temperature distortion across output blackbody aperture and its long term stability.

A rectangular field slit $h \times l = (0.46 \times 8.6)$ mm and input photographic objective select spot size of 1.1×20 mm at an investigated target. As input objective we used low distortion ($< 1.0\%$) objective with focus 135 mm and aperture 1:2.8.

2.1. THE LINE SCANNING PYROMETER DESIGN.

The simplified functional block diagram of the pyrometer for measurement of the brightness temperature distribution during single-crystal growth from a melt is shown in Figure 1. The pyrometer measures brightness temperature at 20 points across melt-crystal interface in narrow bandwidth at the wavelength - $\lambda_p = 0.827 \mu\text{m}$. The objective (2) collects radiation from the opaque melt-crystal boundary (1) and focuses it on the front mat surface of the aperture stop (4) that has a rectangular slit of $h \times l = (0.46 \times 8.6)$ mm. The eyepiece (3) and trunnion-type mirror (8), witch reflect a target image from input aperture stop, are used for the pyrometer focusing and aligning to a target. The radiation passes through the slit of the aperture stop, and is incident on the filter monochromator (5, 6), that used interference filter (5) and focusing lens (6). Monochromatic radiation passed the filter monochromator, is focusing on Si photodiode array (7) that has 20 photodiodes and one temperature sensor. The interference filter and the photodiode array are mounted in precision miniature thermostats to ensure high long time stability of temperature measurements. The miniature thermostats controlled by an internal microprocessor and works at fixed temperature (of about 40°C) with a precision of ± 50 mK. For temperature control of Si array was used semiconductor p-n junction grown together with photodiodes on the same substrate that excludes errors because of temperature gradients in the array metal case and thermostat.

The Si photodiodes transforms the incident monochromatic radiance into photocurrent that is directly proportional of radiance intensity. Level of photocurrent is depends from measuring temperature and change from 150×10^{-12} A to 5200×10^{-12} A for temperature range $800\text{--}1100^\circ\text{C}$. Twenty individual low noise variable gain transimpedance amplifiers were used to converted photocurrents to voltage. The precision integrating switched

transimpedance amplifiers were optimized for a high signal to noise ratio. Gain of transimpedance amplifiers digitally controlled to expand the dynamic range and increase the signal to noise ratio. Low noise, low drift sigma-delta 24-Bit ADCs used in the internal data acquisition system. The delta-sigma architecture is used to guarantee extremely low error temperature drift and dynamic range 24 bits of no missing codes. The gain of the instrumentation amplifier is controlled by a microprocessor in real time depending on the ADC code. Temperature range was shared by two sub-band 800-950 °C and 950-1100 °C, and microprocessor switches gain of transimpedance amplifiers at 3.34 times depending on the sub-band. That optimize signal to noise ratio for whole range of input photocurrent.

The internal data acquisition system includes twenty, precision, wide dynamic range, 24-bit resolution delta-sigma analog-to-digital converters. All twenty ADCs simultaneously start and end their conversion cycles under the microprocessor control. The way system simultaneously measures photocurrents for all twenty channels of the pyrometer. The ADC transmits the conversion results and receives the commands through a two-wire synchronous serial interface. The serial interface allows easy daisy-chaining of multiple ADCs and easy digital isolation from digital circuit by high-speed optocouplers.

The microprocessor collects ADC's output data in series via synchronous serial interface and computes brightness temperatures (according to the Planck's law) in real time. Than through the standard RS232 interface the data are transmitted to Personal Computer. Designed software package used for choose instrument measurement mode, store data on hard disk and calibrate the pyrometer.

2.2. PYROMETER CALIBRATION

The pyrometer calibrated with help of precision blackbody source in the range 800 to 1100 °C that output aperture diameter was 22.2 mm. The pyrometer spot 1.1×20 mm was close to blackbody aperture diameter. And to exclude errors because of edge effect in temperature distribution across blackbody aperture, we calibrate pyrometer 20 times separately for each channel in central point of blackbody aperture. In addition, it is more preferable, because reduce a discrepancy between calibrations for different channels. Accuracy of matching in temperature measurements between channels are defined by the blackbody temperature distortion across output blackbody aperture and its long term stability and was estimated as ±0.25 °C.

On figure 2 is shown line scanning pyrometer calibration layout. The pyrometer was mounted on table with X-Y positioning stages with straight line accuracy 5 microns and one can move it precisely across axis of blackbody.

Pyrometer calibration was carried out in 7 points in step of 50 °C of 800-1100 °C range during a month. Constants of calibration were determined experimentally by comparing the output signal with known temperatures of the blackbodies as measured by a reference pyrometer

An inverse brightness temperature of a black body linearly depends on the logarithm of the photocurrent I (or spectral intensity) by according the Wien radiation law $L_\lambda = c_1 \lambda^{-5} \exp(-c_2 / \lambda T)$ where L_λ is the spectral intensity, λ is the wavelength of

the pyrometer, T is the black body temperature, $c_1 = 2h_P c_0^2$, $c_2 = \frac{h_P c_0}{k_B}$, k_B is Boltzmann constant, h_P – Plank constant; c_0 – velocity of light in vacuum. Experimental data of the pyrometer calibration and liner fit of the data with according of the Wien radiation law presented on figure 3a, the relative error between experimental data and calculation data is shown on figure 3b. Over the range 800 - 1100 °C the relative errors were within 0.1 % that speaks about quality of the carried out calibration. Individual temperature calibrations for each channel have been used for brightness temperature calculation. The tests of pyrometer resolution and long-term drift for all channels were carried out against the blackbody source at temperature 1000 °C. In figure 5 shown blackbody temperature monitoring during 800 sec, the picture show that temperature noise is 0.01 °C and relative temperature drift of the photodiode array thermostat is about ± 0.015 °C with regard to its average temperature. No influence of temperature Si array of pyrometer readings within range of thermostat regulation accuracy. Total value of long-term drift of the pyrometer and the blackbody is than ± 0.2 °C for 8 hours at 1000 °C.

3. BICOLOR PYROMETER FOR MEASUREMENTS OF SUPERCOOLING IN THE MELT CRYSTAL GROWTH.

The pyrometer measures two brightness temperatures and one color in an experimental setup for growth of single crystals. The temperature resolution depends on the measuring temperature, with a typical value of 0.01 °C. Details of the pyrometer design, calibration and performance under actual conditions of dielectric single crystal grows are presented. The performance of the pyrometer is shown in the Table 2.

3.1. THE PYROMETER DESIGN

The developed pyrometer measures spectral radiance temperatures on two wavelengths, which are in the range 0.60 to 1.1 μm . An internal precision digital data acquisition system provides high-resolution temperature measurements with sampling time from 5 to 1000 ms and covers the temperature range of 600 to 1200 °C.

The simplified functional block diagram of the pyrometer is shown in Figure 5. The objective (2) collects radiation from the melt-crystal boundary (1) and focuses it on the front mirror surface of the aperture stop (4) that is used as a pinhole diaphragm. The radiation passes through the hole of the aperture stop, and is incident on the diffraction grating system (5,6). This system achieves high contrast in the narrow spectral bandwidth $\Delta\lambda=30$ to 40 nm. The cut-off filter (7) ($\lambda =750$ nm) reduces high-order spectral components. The lens of the diffraction grating system (5) focuses radiation on the photodiode array (8). The photodiode array is mounted in a miniature thermostat, controlled by an internal microprocessor that works at fixed temperature of about 45 °C with a precision of 0.01 °C. The photodiode transforms the radiance energy into photocurrent that is converted to voltage by a low noise variable gain transimpedance amplifier. The precision integrating switched transimpedance amplifier was optimized for a high signal to noise ratio. The transimpedance amplifier has digitally controlled gain to expand the dynamic range and increase the signal to noise ratio. It integrates the low-level input

current for a determined period to optimize the output voltage level. A low noise, low drift sigma-delta 24-Bit ADC is used in the internal data acquisition system. The gain of the instrumentation amplifier is controlled by a microprocessor in real time depending on the ADC code. Internal memory (RAM) is used for data recording and computing two brightness temperatures (according to the Planck's law) in real time. The pyrometer is controlled (measurement mode, calibration and data storage) by a personal computer through the standard RS232 interface.

3.2. PYROMETER CALIBRATION

The pyrometer was calibrated with help of two blackbody sources in the range 600 to 1200 °C. Calibration constants were determined experimentally by comparing the output signal with known temperatures of the blackbodies as measured by a reference pyrometer [4]. The pyrometer long-term drift testing was carried out against a blackbody source that was based on a sodium heat pipe and that had very small temperature gradients along the radiating cavities. The pyrometer shows a resolution of 0.01 °C for brightness temperature measurements for the blackbody temperature 900 °C, and the long-term drift is less than 0.1 °C for 8 hours.

4. SUPERCOOLING MEASUREMENTS

Experimental data of temperature monitoring during the melting of the sample and its crystallization are shown in Figure 6. The studies performed have allowed to obtain direct data on the dependence of interface supercooling on the single crystal growth rate during its growth from the melt. It has been found that the supercooling of $\text{Bi}_4\text{Ge}_3\text{O}_{12}$ reaches high values (up to 10 K), and depends nonlinearly on the growth rate. This research has shown that experimental conditions can essentially increase the measured value of supercooling when determining supercooling ΔT in measurements of brightness temperature at the interface through the growing crystal with the optical pyrometer. The value of the measurement error depends on the value of absorptivity of the sample and the temperature distribution in the sample, on the length of the sample and on variation of the length during measurements. The procedure of supercooling temperature correction is described in [3].

5. CONCLUSIONS

These in-house designed optical high-resolution pyrometers provide precise measurements of very small temperature variations in modern thermophysical experiments. The pyrometers show high sensitivity, wide temperature span and a response time up to 5 ms that ensure their wide applications in physical experiments. The pyrometers were tested on real experimental setups for interface supercooling measurements on single crystal growth rate from a melt.

ACKNOWLEDGMENTS

The pyrometer for the supercooling measurement development was supported in part by Award No. RE1-2233 of the U.S. Civilian Research & Development Foundation for

the Independent States of the Former Soviet Union (CRDF), in part by INTAS project No. 2000-263, and in part by the Russian Fund of Basic Research (RFBR), Project No. 02-02-17128.

REFERENCES

1. Sentchenko V., Dozhdikov V., Smurov I. et al., "Surface Temperature Monitoring During Pulsed Laser, Electron Beam and Plasma Action," *High Temperature Material Processes* **1**, 109-123 (1997).
2. Sentchenko V., Dozhdikov V., Ignatiev M. and others, *Applied Surface Science* **109/110**, 498-508 (1997).
3. Golyshev V.D., Gonik M.A., and Tsvetovsky V.B., *High Temp.- High Press.* **32**, 581-588 (2000).
4. Saprisky V.I., Khlenov B.B., Khromchenko V.B. et al., in *Proceedings of Tempmeko '96*, eds. P. Marcarino, Levrotto & Bella, Torino, Italy, 1996, pp. 321-326.

Table 1. Specification of the Line Scanning Pyrometer (LSP-I).

Temperature Range, °C	800 ... 1100
Number of brightness channels	20
Working wavelength λ_p , nm	827
Spectral band-width $\Delta\lambda$, nm	26
Instrumental error of brightness temperature measurement, %	0.1
Resolution for a separate brightness channel, mK	20-50
Matching of temperature calibration for channels, °C	± 0.2
Long term stability in 8 hours (at 800... 1100°C), better °C	± 0.2
Distance to object, mm	450 ... 470
Spot size L×W, mm	1.1x20
Photo Detector temperature stabilization, better mK	± 50
The measuring time, s	0.1-30
Type of interface	RS232
Data transfer rate, kbaud	9.6 – 115.2
Warming-up time, min	30
Power consumption, W	20
Weight, kg	4.0
Dimensions, mm	170×205×530

Table 2. Specification of the bicolour pyrometer.

Temperature range, °C	600 to 1200
Temperature resolution, mK	10-50
Working wavelengths λ_1 , nm λ_2 , nm	795 995
Spectral band-width $\Delta\lambda_1$ $\Delta\lambda_2$, nm	30/40
Instrumental error of brightness temperatures measurement, %	± 0.15
Working distance L , mm	400 to 450
Field of view, \varnothing mm	1
The measuring time, ms	5 to 1000
Type of interface	RS232
Data transfer rate, kbaud	9.6 to 115.2
Weight, kg	4.5
Dimensions, mm	270×150×240

FIGURE 1. Simplified block diagram of the line scanning pyrometer.

1 - growing semi-transparent single-crystal; 2 - objective; 3 - microscope eyepiece; 4 - precision slit $h \times l = (0.46 \times 8.6)$ mm; 5 - broadband interference filter in thermostat $\lambda_p = 827$ nm, $\Delta\lambda_{0.5} = 26$ nm; 6 - IR objective; 8 - Si twenty-photodiode array in thermostat.

FIGURE 2. Line Scanning Pyrometer calibration layout.

FIGURE 3. a) Experimental calibration data (\square) and liner fit (-) of the data; b) Relative error of calibration for individual channel of the pyrometer.

FIGURE 4. The result of the temperature resolution tests of the pyrometer.

FIGURE 5. Simplified block diagram of the pyrometer. 1 - growing semi-transparent single-crystal; 2 - low distortion objective; 3 - microscope eyepiece; 4 - precision mirror slit $\varnothing = 0.5$ mm; 5 - lenses of grating monochromator; 6 - grating 600 l/mm; 7 - cutoff filter 750 nm; 8 - Si photodiodes array in thermostat.

FIGURE 6. Monitoring of the sample temperature during its melting and crystallization.

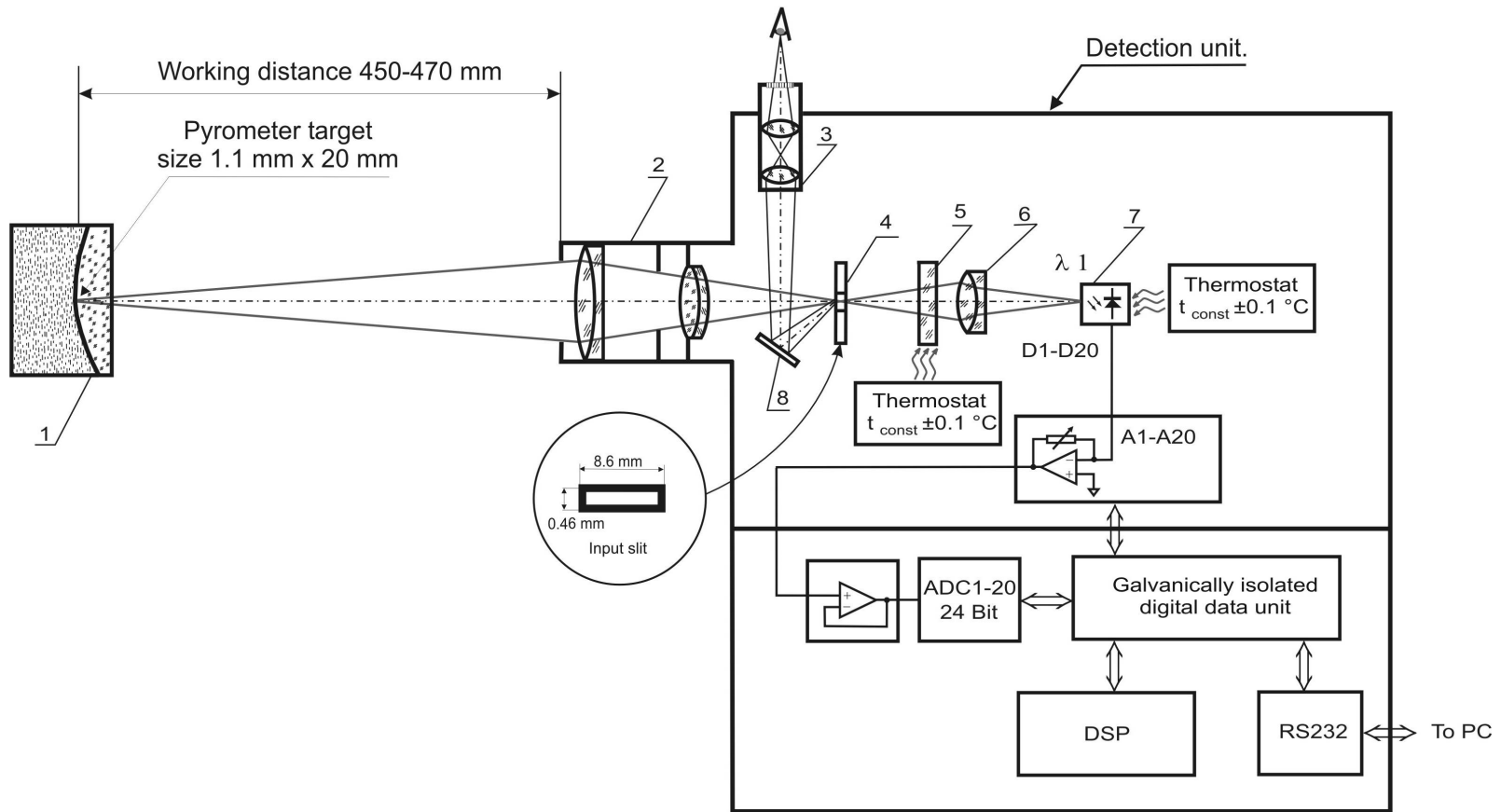


FIG. 1

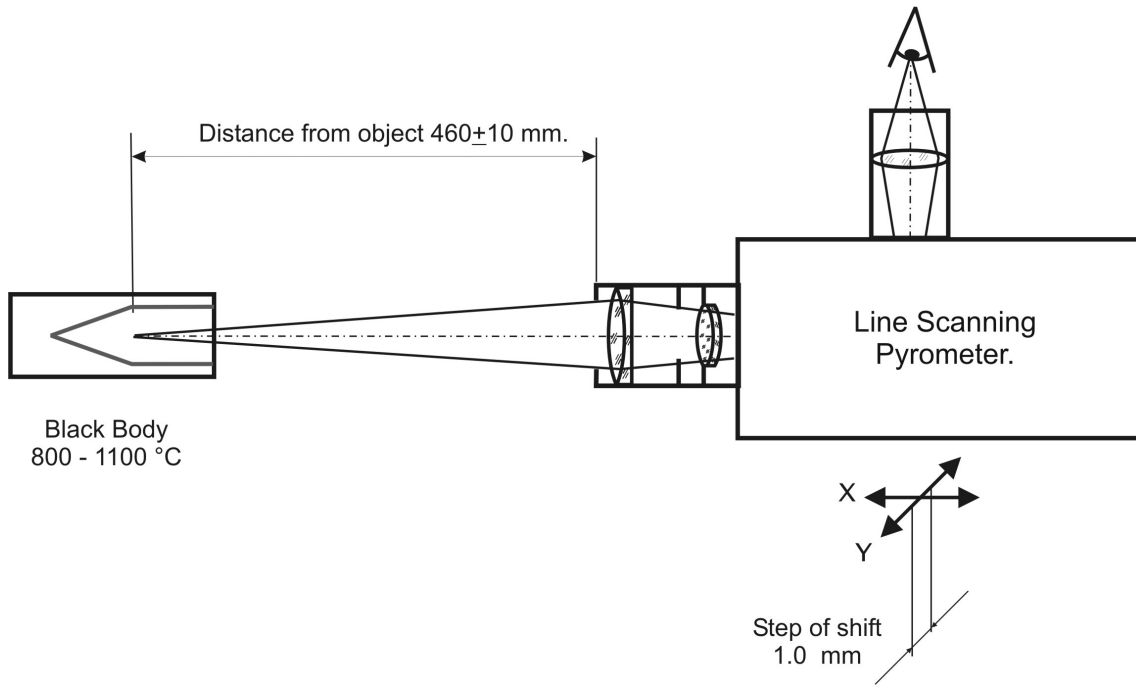
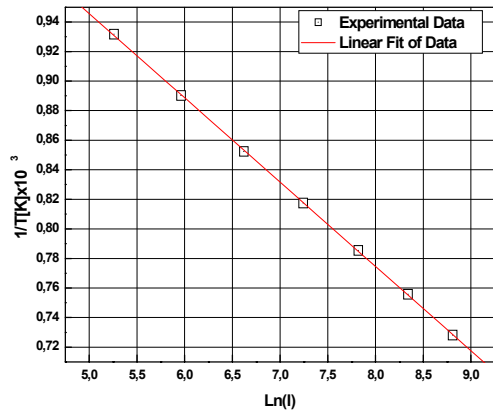
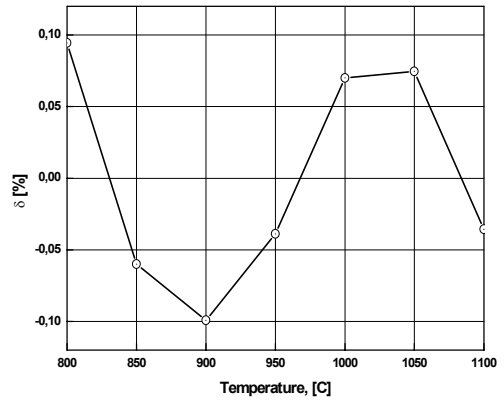


FIG. 2



a)



b)

FIG. 3

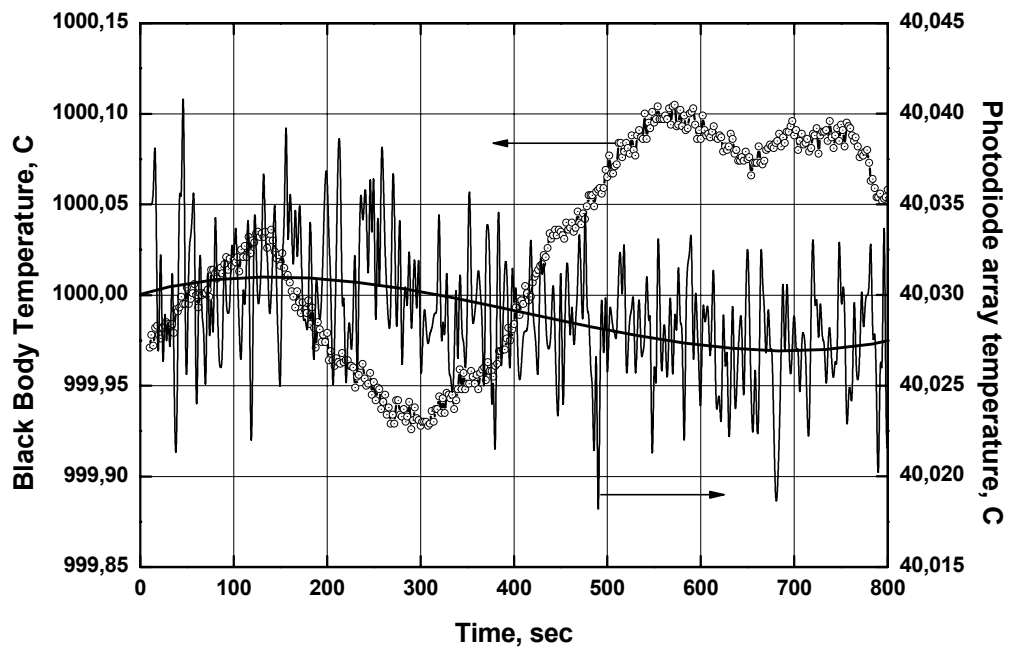


FIG. 4

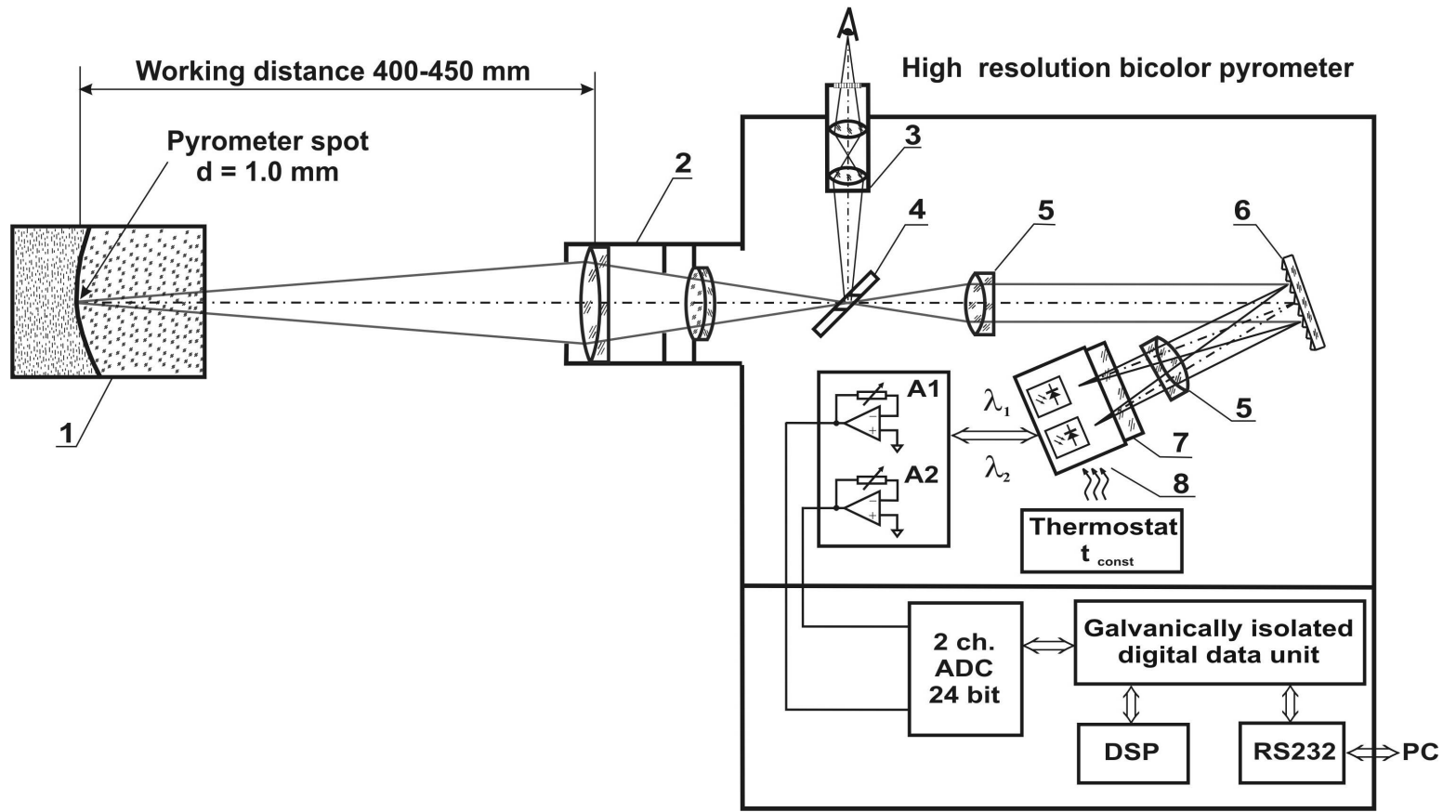


FIG. 5

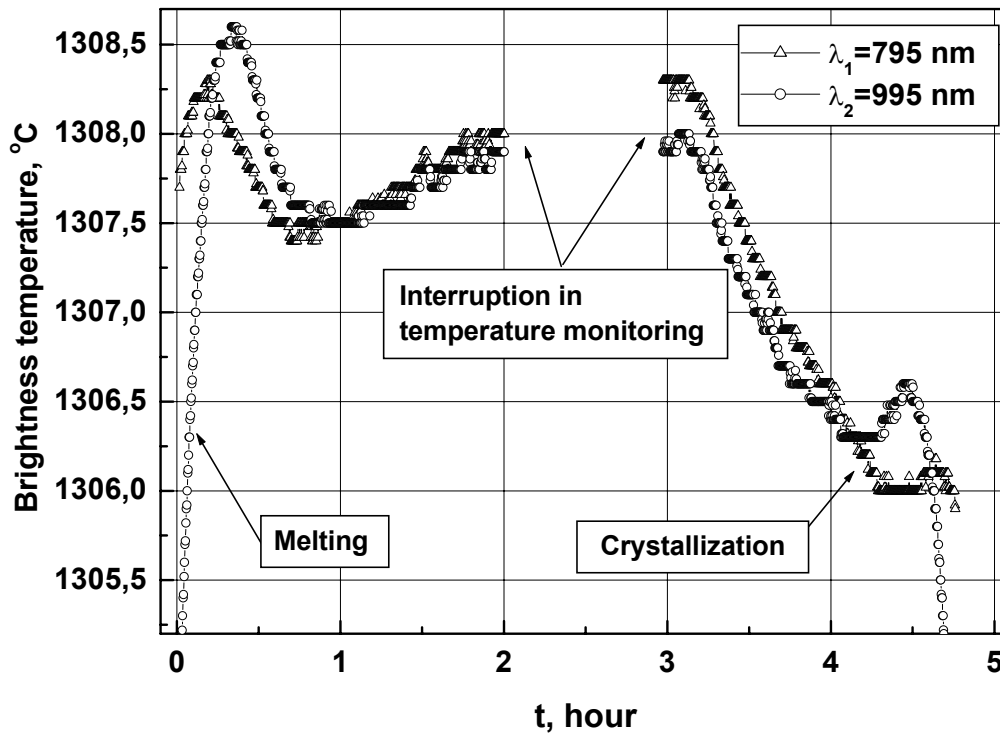


FIG. 6